Proc. Natl. Acad. Sci. USA
Vol. 87, pp. 9645–9649, December 1990
Botany

Effects of auxin and abscisic acid on cytosolic calcium and pH in plant cells

(plant hormones/confocal scanning optical microscopy/2,4-dichlorophenoxyacetic acid)

CHRISTOPH A. GEHRING, HELEN R. IRVING, AND ROGER W. PARISH

Department of Botany and Centre for Protein and Enzyme Technology, La Trobe University, Bundoora, Victoria 3083, Australia

Communicated by Rutherford N. Robertson, September 4, 1990 (received for review May 4, 1990)

ABSTRACT **Dark-grown corn coleoptiles and parsley hypocotyls and their roots were loaded with acetoxymethyl esterified forms of the Ca^{2+} indicator fluo-3, and the pH indicator 2′,7′-bis(2-carboxyethyl)-5(and -6)-carboxyfluorescein. These tissues were treated with the plant growth regulator 2,4-dichlorophenoxyacetic acid (2,4-D), an auxin analogue, or abscisic acid (ABA), and the cytosolic pH (pH_{cyt}) and cytosolic Ca^{2+} ($[Ca^{2+}]_{cyt}$) changes were monitored by confocal scanning optical microscopy. Over a period of 4 min pH_{cyt} decreased 0.1–0.2 pH unit and $[Ca^{2+}]_{cyt}$ increased from 280 to 380 nM in response to 2,4-D. ABA, on the other hand, induced cytosolic alkalinization of 0.05–0.1 pH unit with a concomitant increase in $[Ca^{2+}]_{cyt}$ from 240 to 320 nM over a 4-min period. Responses similar to these were observed in all the tissues tested. We suggest that pH_{cyt} profoundly influences signaling by $[Ca^{2+}]_{cyt}$, possibly by regulating Ca^{2+}–protein binding, and that the divergent effects of auxin and ABA on pH_{cyt} underlie their mutual antagonism.**

The plant growth regulators auxin (IAA; indoleacetic acid) and abscisic acid (ABA) influence plant development in a variety of ways. IAA, for example, promotes cell enlargement, cell division, vacuolar tissue differentiation, and tropistic responses (1). ABA enhances adaptation to various stresses and is involved in, for example, water regulation, photosynthate transport, and induction of seed storage protein synthesis (1, 2). ABA and IAA effects can be antagonistic. ABA inhibits IAA-induced cell elongation (3) and IAA can reverse the inhibitory effect of ABA on stomatal opening (4).

Our work aims to identify the early messengers in IAA and ABA action. We found that application of IAA to corn coleoptiles led to rapid cytosolic acidification of epidermal cells (5). Acidification was monitored with a pH-sensitive microelectrode and was detectable <5 min after IAA was added. A decrease of ≈0.1 pH unit occurred and the cytosolic pH (pH_{cyt}) began to oscillate with a period of 20–30 min (5). Microelectrode studies showed IAA also rapidly increased cytosolic free Ca^{2+} ($[Ca^{2+}]_{cyt}$) levels, which oscillate with changes in pH_{cyt} (6). The pH_{cyt} decrease may be responsible for the increase in $[Ca^{2+}]_{cyt}$ (7). We have found that increased $[Ca^{2+}]_{cyt}$ and decreased pH_{cyt} are spatially correlated with the localized increases in cell elongation associated with geo- and phototropisms of corn coleoptiles (8). Stomatal closure is induced by ABA (4) and appears to be dependent on the availability of Ca^{2+} (9). However, no consistent effect on guard cell $^{45}Ca^{2+}$ uptake was seen in response to ABA application (10). No response to ABA was seen in $[Ca^{2+}]_{cyt}$ in root hairs injected by iontophoresis with the Ca^{2+} probe fura-2 (11). In contrast, ABA was shown to cause a transient increase in $[Ca^{2+}]_{cyt}$ in guard cells prior to closure (12).

In this paper, we use confocal scanning optical microscopy (CSOM) to compare the effects of 2,4-dichlorophenoxyacetic acid (2,4-D) and ABA on pH_{cyt} and $[Ca^{2+}]_{cyt}$. Both growth regulators were found to increase $[Ca^{2+}]_{cyt}$ rapidly in all tissues studied. However, whereas IAA lowered pH_{cyt}, pH_{cyt} was raised by ABA.

MATERIALS AND METHODS

Plant Material. *Zea mays* (Terrific) seeds were soaked for 8–12 hr in tap water. They were then placed in moist vermiculite in a plastic box for 4–5 days at 26°C in the dark. The apical 3 mm of the coleoptile was removed, the following 10–20 mm was excised, and the primary leaves were removed. The coleoptile or roots were then cut into segments 1–4 mm long. Parsley (*Petroselinum hortense*) seeds were planted directly into a moist vermiculite/sand mixture (2:1) and incubated in the dark at 26°C for 6–9 days. Hypocotyls or roots were also cut in segments 2–4 mm long.

Dye Loading. Plant segments were loaded with fluorescent probes by incubation with the acetoxymethyl esterified forms of the Ca^{2+} indicator fluo-3 (Molecular Probes), or the pH indicator 2′,7′-bis(2-carboxyethyl)-5(and -6)-carboxyfluorescein (BCECF) (Molecular Probes), for 1 hr at 26°C in the dark. The final dye concentration was 0.25–0.5 μM in tap water. Dye loading was terminated by rinsing the plant material in tap water. Results from preliminary experiments were similar to those presented (see Figs. 1–4); however, fluo-3 uptake into cells of plant segments was facilitated by removal of the waxy cuticle with adhesive tape (8, 13) and by incubating in the presence of 0.02–0.2% of the nonionic, low toxicity detergent Pluronic F-127. Fluo-3 uptake into parsley hypocotyl tissue segments was further enhanced by exposing the vertical sections to 15,000 × *g* for 30 s to 3 min in the presence of dye and detergent prior to incubation in the dark. The tissue segments grew in response to IAA after loading with fluo-3. Growth of IAA-stimulated coleoptile segments was inhibited by ABA (data not shown).

CSOM. Coleoptile and hypocotyl segments loaded with fluo-3/AM or BCECF/AM were placed on a glass slide to view either longitudinal or cross-sections with a Nikon optiphot microscope. Intracellular fluorescence was excited with the 488-nm band of an argon-ion laser scanned through the computer-controlled galvanometer mirrors of a laser scan confocal microscope (Lasersharp MRC-500, Bio-Rad). The average number of scans collected per image (time point) was 11 or 12 and remained unchanged throughout the experiment. Further details of image acquisition have been described (13). Prints were generated with a Mitsubishi video image processor. Photobleaching and dye leakage controls were made by comparing average cellular fluorescence intensities of

The publication costs of this article were defrayed in part by page charge payment. This article must therefore be hereby marked "*advertisement*" in accordance with 18 U.S.C. §1734 solely to indicate this fact.

Abbreviations: 2,4-D, 2,4-dichlorophenoxyacetic acid; ABA, abscisic acid; BCECF, 2′,7′-bis(2-carboxyethyl)-5(and -6)-carboxyfluorescein; $[Ca^{2+}]_{cyt}$, cytosolic free Ca^{2+}; CSOM, confocal scanning optical microscopy; IAA, auxin; pH_{cyt}, cytosolic pH.

scanned and adjacent areas at the end of each experiment. The degree of photobleaching was dependent on the gain of the argon laser and was more marked when the tissue segments were poorly loaded. If the combined levels of photobleaching and dye leakage exceeded 15% of the fluorescence intensity over 10 min, the experiment was discarded. The plant segments depicted in Figs. 2–4 contain some cells with little fluorescence as the optical section passed through the vacuole. This suggests that the majority of BCECF/AM and fluo-3/AM is cleaved and remains in the cytosol (as discussed in ref. 13). The heterogeneity of fluorescence intensities between cells is caused by differences in the thickness of the layer of cytosol surrounding organelles (e.g., the vacuole) from which dye is excluded (13). Changes in pH_{cyt} and $[Ca^{2+}]_{cyt}$ can only be calculated from cells with the cytosol fully in the focal plane. It is difficult to monitor cells accurately for >15 min by CSOM. When collecting a series of images during time course experiments, changes in focal plane, photobleaching, dye leakage (especially from the surface cells), and dehydration may interfere with accurate monitoring of fluorescent changes. In plant tissues, changes in focal plane are detected by movement of highly autofluorescent plastids in and out of focus. Fluorescent changes in opposite directions in neighboring cells are more probably caused by specimen movement and reflect changes in focal plane rather than ion activity.

Calibration of Calcium and pH Levels. No spectral shift occurs upon the binding of cations with fluo-3. Therefore, Ca^{2+} levels have to be estimated by ionophore addition to determine fluorescence limits (14). The upper fluorescent limit (F_{max}) is determined by addition of Ca^{2+} to saturate the dye in the cytoplasm. The lower limit (F_{min}) is established by the addition of Mn^{2+}, which displaces Ca^{2+} from the dye and thereby quenches its fluorescence. $[Ca^{2+}]_{cyt}$ was then calculated from the equation $[Ca^{2+}] = K_d(F\text{-}F_{min})/(F_{max} - F)$, where K_d is ≈400 nM and the fluorescence enhancement of fluo-3 on Ca^{2+} binding is ≈36-fold (13, 14). As a single wavelength mode was used, the BCECF fluorescence cannot be directly quantitated *in vivo*. However, the *in vivo* responses to the dye were ascertained by brief exposure to procaine (100 mM), which induces alkalization, and to fusicoccin (0.73 mM), which lowers pH_{cyt} (5) and quenches the dye signal. Furthermore, fluorescence maxima and minima were established in the presence of the H^+/K^+ exchanger nigericin, plus alkali (pH 8.1) or acid (pH 5.8) potassium phosphate buffers (15). Changes in pH_{cyt} can be calculated because a linear relationship exists between pH and fluorescence intensities over the pH range 6.4–7.6 (15). The K_d of BCECF is 10^{-7} and fluorescence decreases 3-fold upon H^+ association (15).

RESULTS

Effects of 2,4-D and ABA on pH_{cyt}. The addition of 2,4-D to hypocotyl, coleoptile, or root segments results in cytosolic acidification of between 0.1 and 0.2 pH unit (a decrease in fluorescence intensity of BCECF). This was observed in eight of eight successful experiments in which segment movement, photobleaching, and dye leakage were eliminated. The decrease was always observed to begin within the first minute. This is shown in Fig. 1 where 2,4-D was added as a 1-μl drop of a 100 μM solution to the surface of the parsley segment. The drop was added and then removed after 5 s to allow image collection. Similar effects were observed with 1 μM 2,4-D when it was added to plant segments submerged in 100 μl of tap water. However, additions to submerged tissues often lead to segment movement and concomitant changes in focal plane, thereby distorting the results. At the end of the experiments, the magnification of the computer-generated image was reduced to allow comparisons of fluorescence intensity between scanned and adjacent areas to ensure that photobleaching of the dye had not been caused by the laser beam (see Fig. 1*i*). The results indicated that a decrease in dye fluorescence intensity had occurred throughout the segment and therefore the acidification that this indicates was genuine. Coleoptile cross-sections responded to 2,4-D or IAA with a decrease of pH_{cyt} of nearly 0.3 unit over 6 or 9 min, respectively. A decrease of only 0.1 pH unit was observed in a parsley root segment in response to 2,4-D (data not shown).

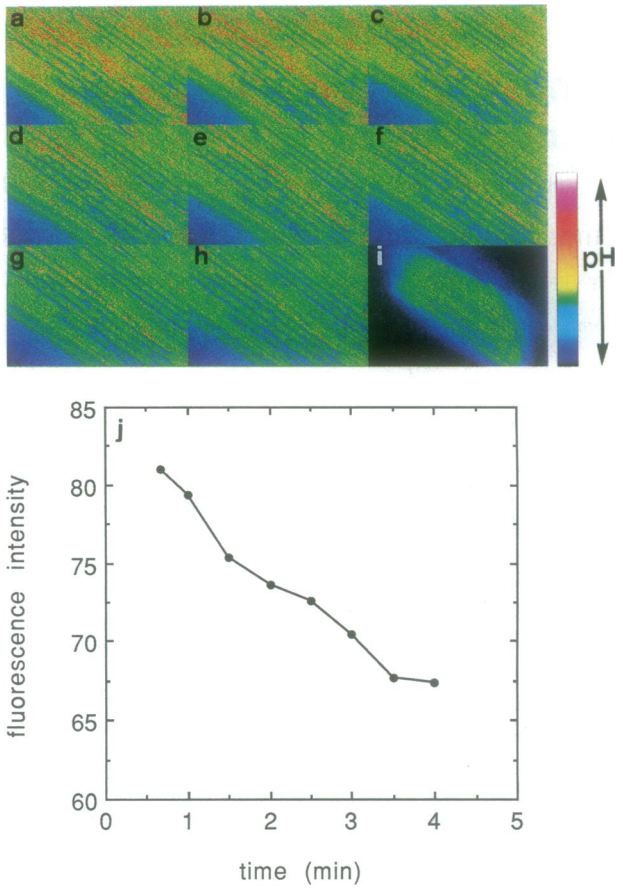

FIG. 1. Changes in pH_{cyt} in response to 2,4-D of parsley hypocotyl. Fluorescence video images of a longitudinal section of a parsley hypocotyl loaded with BCECF after a 5-s application of a 1-μl drop of 100 μM 2,4-D to the surface of the segment. The images are an average of 11 scans at each time point and were taken at the following times after 2,4-D application: *a*, 40 s; *b*, 1 min; *c*, 1.5 min; *d*, 2 min; *e*, 2.5 min; *f*, 3 min; *g*, 3.5 min; *h*, 4 min; *i*, 4.3 min (an average of 12 scans as a photobleach control). (*j*) Time plot of the BCECF fluorescence intensity (arbitrary units) for the video images in *a–h*. The color bar represents a pH range from 5.8 (pale blue) to 8 (pink). (*a–h*, ×50; *i*, ×20.)

Since epidermal cells are less vacuolated and more readily accessible to the dye during loading, they generally emit more fluorescence than cortical cells. For this reason, fluorescence responses of these two cell types should not be quantitatively compared. However, the direction of fluorescence changes after stimulation with 2,4-D is the same in both cell types. Cytosolic acidification was also observed in seven of eight successful experiments after addition of fusicoccin and no change was observed in the eighth trial. The brief (5 s) addition of 70 μM fusicoccin caused a cytosolic acidification of 0.1 pH unit, whereas a 0.7 mM addition caused a decrease in pH_{cyt} of 0.2 unit within 4 min (data not shown). The degree of acidification observed (0.1–0.2 pH unit) in response to 2,4-D and fusicoccin with CSOM is very similar to that found by using microelectrodes (5, 7).

Addition of a 2-μl drop of 10 or 100 μM ABA to tissue segments led to a cytosolic alkalization of 0.05 to 0.2 pH unit in 11 of 11 trials. This is illustrated in Fig. 2, where a corn coleoptile segment is briefly exposed to a drop of 100 μM ABA and the change in BCECF fluorescence intensity was monitored for the next 3 min. The change in this instance was $\approx$0.2 pH unit. At the end of the experiment, the H^+/K^+ exchanger nigericin was added and the minimum and maximum fluorescence were observed at pH 5.8 (Fig. 2*h*) and at pH 8 (Fig. 2*i*), respectively. In two other cases, ABA was observed to raise pH_{cyt} $\approx$0.2 unit in a coleoptile and corn root over a 12- and 6-min period, respectively. In a parsley hypocotyl, the response was less with pH_{cyt}, increasing 0.1 pH unit over 6 min (data not shown).

Effects of 2,4-D and ABA on $[Ca^{2+}]_{cyt}$. $[Ca^{2+}]_{cyt}$ increased on addition of 2,4-D in coleoptiles (Fig. 3) and also in hypocotyl and root segments (data not shown). Again the plant hormone was applied as a drop to the surface of the tissue segment and was removed 5–10 s after application. The first image was acquired 10 s after addition of 2,4-D (Fig. 3) and the mean $[Ca^{2+}]_{cyt}$ was 280 nM. Fluorescence increased over the imaging period, with $[Ca^{2+}]_{cyt}$ reaching 380 nM by 4 min. When 2,4-D was added to a parsley hypocotyl, $[Ca^{2+}]_{cyt}$ increased from 85 nM at 30 s to 230 nM at 6.5 min (data not shown). In several instances, the effect of 2,4-D was slight over the time period observed, which could be due to

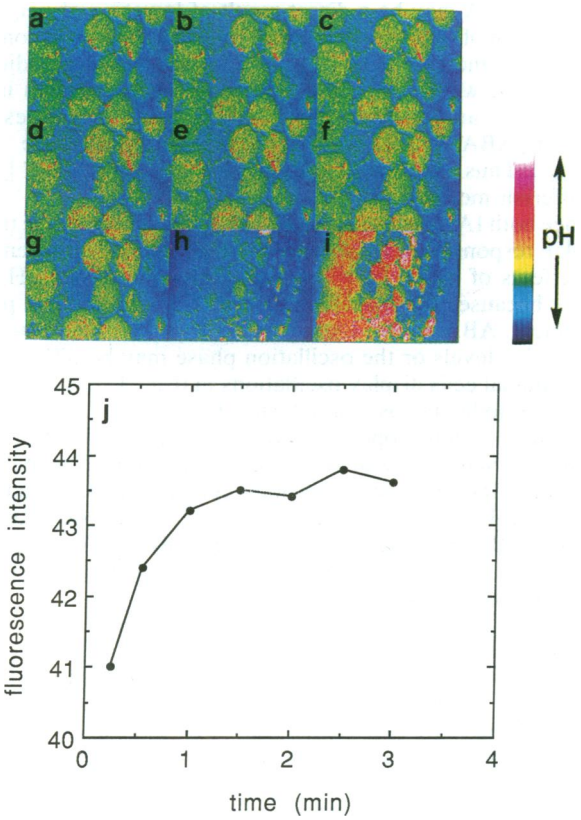

FIG. 2. Changes in pH_{cyt} in response to ABA of corn coleoptile. Fluorescence video images of a cross-section of a coleoptile loaded with BCECF after a 5-s application of a 2-μl drop of 100 μM ABA to the surface of the segment. The images are an average of eight scans at each time point and were taken at the following times after ABA application: *a*, 15 s; *b*, 35 s; *c*, 1 min; *d*, 1.5 min; *e*, 2 min; *f*, 2.5 min; *g*, 3 min; *h*, 15 s after adding nigericin and potassium phosphate buffer (pH 5.8); *i*, 15 s after raising the pH to 8.1 with potassium phosphate buffer. (*j*) Time plot of the BCECF fluorescence intensity (arbitrary units) of the video images in *a*–*g*. The color bar represents a pH range from 5.8 (pale blue) to 8 (red). (*a*–*g*, ×70; *h* and *i*, ×50.)

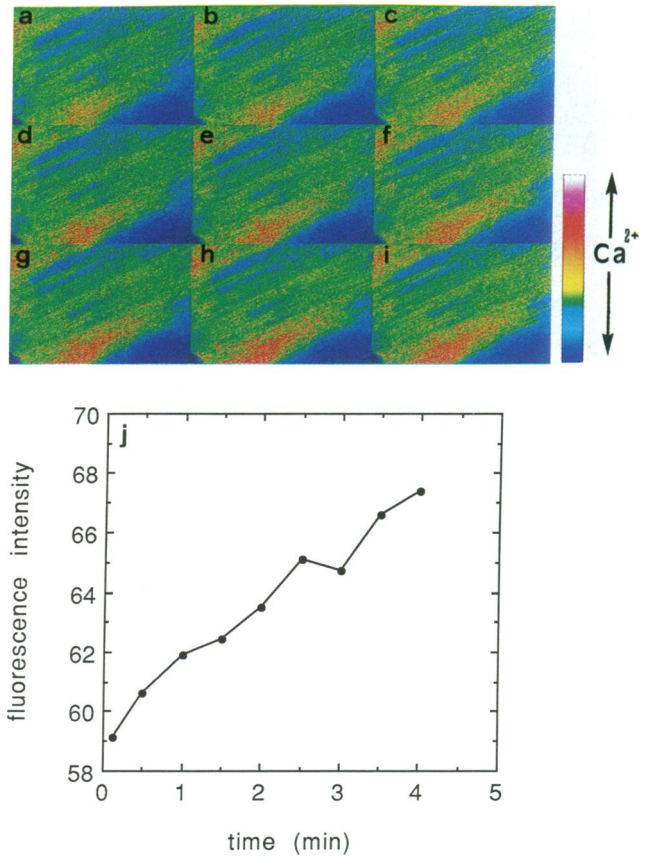

FIG. 3. Changes in $[Ca^{2+}]_{cyt}$ in response to 2,4-D of a corn coleoptile. Fluorescence video images of a longitudinal section of a coleoptile loaded with fluo-3 after a 5-s application of 1 μl of 100 μM 2,4-D to the surface of the segment. The images are an average of 11 scans at each time point and were taken at the following times after 2,4-D application: *a*, 10 s; *b*, 30 s; *c*, 1 min; *d*, 1.5 min; *e*, 2 min; *f*, 2.5 min; *g*, 3 min; *h*, 3.5 min; *i*, 4 min. (*j*) Time plot of the fluo-3 fluorescence intensity (arbitrary units) of the video images in *a*–*i*. The color bar represents a range of $[Ca^{2+}]$ from 10 nM (pale blue) to 40 μM (pink-white). (×30.)

incomplete penetration of the growth regulator. The data were unreliable over longer periods as the tissue segments tended to dry out and cause changes in the focal plane.

The addition of a 2-μl drop of 100 μM ABA to a corn root segment resulted in $[Ca^{2+}]_{cyt}$ increasing from 240 nM at 40 s to 320 nM over the 4-min imaging period (Fig. 4). When a drop of 10 μM ABA was in contact with a root segment for 5 s the level of $[Ca^{2+}]_{cyt}$ increased from a basal level of 100 nM to 150 nM within 5 min. A similar result was observed after addition of ABA to a coleoptile segment where $[Ca^{2+}]_{cyt}$ increased from 120 nM to 150 nM within 4 min. The addition of ABA to a parsley hypocotyl resulted in the $[Ca^{2+}]_{cyt}$ increasing from 300 nM at 1 min to 590 nM in the next 2 min (data not shown). Increases in $[Ca^{2+}]_{cyt}$ in response to ABA were observed in seven of eight successful measurements and no change was observed in the other experiment.

In the experiments presented, the basal levels of $[Ca^{2+}]_{cyt}$ ranged from 100 to 300 nM. These values are comparable to those determined with double-barreled Ca^{2+} microelectrodes (6, 7) as well as those obtained using electropermeabilized protoplasts loaded with the fluorescent dye Quin-2 (16). This was also seen in *Chara* cells microinjected with aequorin where basal levels of $[Ca^{2+}]_{cyt}$ ranged from 100 to 560 nM (17). In root hairs (11) microinjected with fura-2, the $[Ca^{2+}]_{cyt}$ ranged from 30 to 90 nM, whereas *Fucus* rhizoids had levels ranging from 105 to 450 nM (18). Similarly, guard cells iontophoretically injected with fura-2 had resting $[Ca^{2+}]_{cyt}$

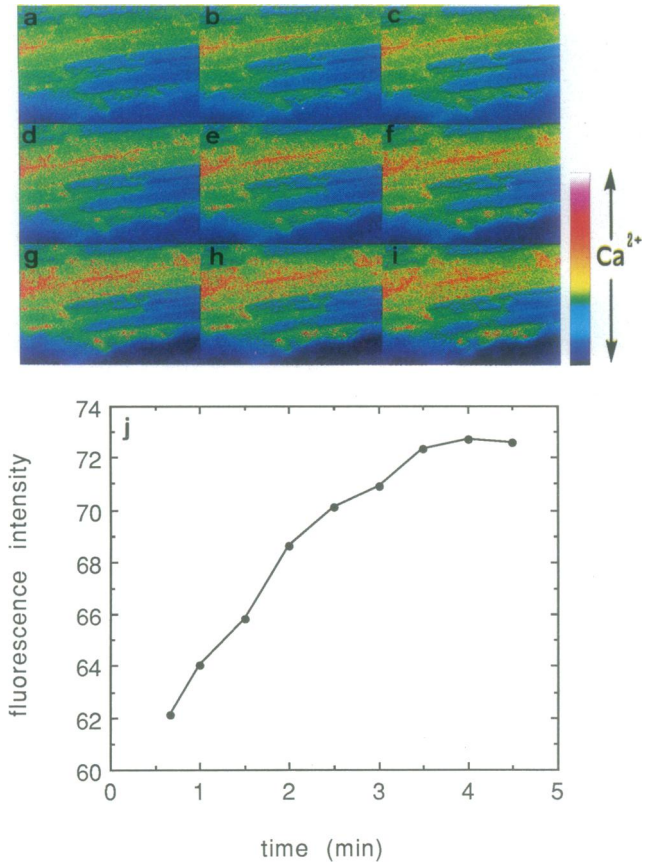

FIG. 4. Changes in $[Ca^{2+}]_{cyt}$ in response to ABA of a corn root. Fluorescence video images of a longitudinal section loaded with fluo-3 after a 5-s application of 2-μl of 100 μM ABA to the root surface. The images are an average of 12 scans at each time point and were taken at the following times after ABA application: *a*, 40 s; *b*, 1 min; *c*, 1.5 min; *d*, 2 min; *e*, 2.5 min; *f*, 3 min; *g*, 3.5 min; *h*, 4 min; *i*, 4.5 min. (*j*) Time plot of fluo-3 fluorescence intensity (arbitrary units) of the video images in *a–i*. The color bar represents a range of $[Ca^{2+}]$ from 10 nM (pale blue) to 40 μM (pink-white). (×70.)

ranging from 70 to 250 nM (12). Incremental changes of $[Ca^{2+}]_{cyt}$ in response to IAA are similar to those measured with microelectrodes (6).

DISCUSSION

Our results confirm earlier work that IAA rapidly lowers the pH_{cyt} (5, 6, 19) and increases the levels of $[Ca^{2+}]_{cyt}$ (6) in corn coleoptile cells. The original work was done with microelectrodes and, hence, was restricted to measuring changes in a single epidermal cell. CSOM has the advantage that changes in many cells and in neighboring tissues can be measured simultaneously and noninvasively. Small changes in pH_{cyt} or $[Ca^{2+}]_{cyt}$ can be monitored within 30 s of the addition of the plant growth regulators. The earlier work with microelectrodes showed that IAA induces oscillations in membrane potential, pH_{cyt}, and $[Ca^{2+}]_{cyt}$ with a period of 20–30 min (5, 6).

IAA causes a decrease in pH_{cyt} and an increase in $[Ca^{2+}]_{cyt}$ in all the tissues we have so far studied (corn coleoptiles, parsley hypocotyls, corn and parsley roots). Hence, the inhibitory effects of IAA on the growth of excised (20, 21) and intact (22) roots cannot result from an inability of the growth regulator to modify pH_{cyt} or $[Ca^{2+}]_{cyt}$ levels.

Recent work indicated that IAA added to excised pea internodes rapidly stimulates the synthesis of wall matrix polysaccharides in the epidermal but not the cortical cells (23). Assuming the increase in the synthesis of the noncellulosic matrix increases the plasticity of the epidermal wall, these results are consistent with the hypothesis that the epidermis is the primary IAA-sensitive growth-limiting tissue, growth being driven by the compressed inner cells (24, 25). However, we observed no differences in the response of coleoptile epidermal and cortical cells to IAA as reflected in pH_{cyt} and $[Ca^{2+}]_{cyt}$ changes. Consequently, a process further along the signal transduction pathway may be involved in these tissue differences.

In contrast to IAA, ABA was found to increase rapidly the pH_{cyt} of all cells studied (coleoptiles, hypocotyls, and roots). ABA has been shown to reduce the IAA-induced acidification of cell walls, and this was interpreted as ABA inhibition of the proton pump (26, 27). However, our results suggest that the increased and decreased proton excretion caused by IAA and ABA, respectively, reflects changes in pH_{cyt} rather than direct effects on the proton pump. ABA and IAA are known to be antagonistic to one another. IAA, for example, stimulates the opening of stomata and can modify the inhibitory effect of ABA on stomatal opening (4, 28, 29). IAA-mediated elongation of grass coleoptiles is rapidly inhibited by ABA (3, 30, 31). The basis of this antagonism may lie, at least in some cases, in the opposing effects of the two hormones on pH_{cyt}.

The $[Ca^{2+}]_{cyt}$ levels are increased by IAA and ABA in all tissues we have so far examined. The increase in $[Ca^{2+}]_{cyt}$ caused by IAA may be a direct result of lowering of pH_{cyt}. Acidification of the cytosol induced by weak acids is accompanied by an increase in $[Ca^{2+}]_{cyt}$ (7). Microelectrode studies indicate that weak bases (e.g., procaine, methylamine) increase pH_{cyt} and decrease the $[Ca^{2+}]_{cyt}$ (7). Nevertheless, although ABA increases pH_{cyt} there is an increase in $[Ca^{2+}]_{cyt}$. Thus, ABA and IAA apparently increase $[Ca^{2+}]_{cyt}$ by different mechanisms.

Since both IAA and ABA raise $[Ca^{2+}]_{cyt}$ levels, why are the cellular responses to these growth regulators so different? The effects of higher $[Ca^{2+}]_{cyt}$ may differ at various pH_{cyt} values because, for example, protein–Ca^{2+} binding is pH dependent. ABA, unlike IAA, may fail to induce oscillations in $[Ca^{2+}]_{cyt}$ levels or the oscillation phase may be different. Many animal cells display oscillations in $[Ca^{2+}]_{cyt}$ as a result of the periodic release of internal Ca^{2+} (32). Oscillation frequency is often proportional to the agonist concentration and so frequency may provide a digital readout of stimulus strength. Moreover, since various cellular functions have different calcium sensitivities, varying the frequency could result in different cellular responses. Finally, ABA and IAA may cause different distributions of the calcium signal in place and time within a single cell.

Recently, McAinsh *et al.* (12) found a rapid and extensive increase in $[Ca^{2+}]_{cyt}$ in response to ABA in guard cells. This change in $[Ca^{2+}]_{cyt}$ of 2- to 10-fold was monitored by dual wavelength epifluorescence microscopy after microinjection of fura-2 into single guard cells. Our work suggests that many different plant cells respond to ABA in a similar fashion.

We wish to thank the John Curtin School of Medical Research, Australian National University, for their hospitality and Ailsa Rolinson for her invaluable assistance with the confocal microscope. We thank Trevor Phillips for processing the photographic material. H.R.I. is supported by an Australian Research Council Research Fellowship.

1. Davies, P. J. (1987) in *Plant Hormones and their Role in Plant Growth and Development*, ed. Davies, P. J. (Martinus Nijhoff, Dordrecht, The Netherlands), pp. 1–12.
2. Zeevaart, J. A. D. & Creelman, R. A. (1988) *Annu. Rev. Plant Physiol. Plant Mol. Biol.* **34**, 439–472.
3. Kutschera, U. & Schopfer, P. (1986) *Planta* **167**, 527–535.
4. Mansfield, T. A. (1987) in *Plant Hormones and their Role in*

Plant Growth and Development, ed. Davies, P. J. (Martinus Nijhoff, Dordrecht, The Netherlands), pp. 411–430.
5. Felle, H., Brummer, B., Bertl, A. & Parish, R. W. (1986) *Proc. Natl. Acad. Sci. USA* **83,** 8992–8995.
6. Felle, H. (1988) *Planta* **174,** 495–499.
7. Felle, H. (1988) *Planta* **176,** 248–255.
8. Gehring, C. A., Williams, D. A., Cody, S. H. & Parish, R. W. (1990) *Nature (London)* **345,** 528–530.
9. De Silva, D. L. R., Hetherington, A. M. & Mansfield, T. A. (1985) *New Phytol.* **100,** 473–482.
10. MacRobbie, E. A. C. (1989) *Planta* **178,** 231–241.
11. Clarkson, D. T., Brownlee, C. & Ayling, S. M. (1988) *J. Cell Sci.* **91,** 71–80.
12. McAinsh, M. R., Brownlee, C. & Hetherington, A. M. (1990) *Nature (London)* **343,** 186–188.
13. Williams, D. A., Cody, S. H., Gehring, C. A., Parish, R. W. & Harris, P. J. (1990) *Cell Calcium* **11,** 291–297.
14. Kao, J. P. Y., Hartootunian, A. T. & Tsien, R. Y. (1989) *J. Biol. Chem.* **264,** 8179–8184.
15. Rink, T. J., Tsien, R. Y. & Pozzan, T. (1982) *J. Cell Biol.* **95,** 189–196.
16. Gilroy, S., Hughes, W. A. & Trewavas, A. J. (1989) *Plant Physiol.* **90,** 482–491.
17. Williamson, R. E. & Ashley, C. C. (1982) *Nature (London)* **296,** 647–651.
18. Brownlee, C. & Pulsford, A. L. (1988) *J. Cell Sci.* **91,** 249–256.
19. Brummer, B., Bertl, A., Potrykus, I. & Parish, R. W. (1985) *FEBS Lett.* **198,** 104–114.
20. Chadwick, A. W. & Burg, S. P. (1967) *Plant Physiol.* **42,** 415–420.
21. Chadwick, A. W. & Burg, S. P. (1970) *Plant Physiol.* **45,** 192–200.
22. Eliasson, L., Bertell, G. & Bolander, E. (1989) *Plant Physiol.* **91,** 310–314.
23. Kutschera, U. & Briggs, W. R. (1987) *Proc. Natl. Acad. Sci. USA* **84,** 2747–2751.
24. Kutschera, U. & Schopfer, P. (1986) *Planta* **169,** 437–442.
25. Kutschera, U. & Briggs, W. R. (1987) *Plant Physiol.* **84,** 1361–1366.
26. Schubert, S. & Matzke, H. (1985) *Physiol. Plant.* **64,** 285–289.
27. Petzold, U., Dahse, I. & Jacob, F. (1988) *Biol. Plant.* **30,** 252–259.
28. Pemadasa, M. A. (1982) *New Phytol.* **90,** 209–219.
29. Snaith, P. J. & Mansfield, T. A. (1982) *Plant Cell Environ.* **5,** 309–311.
30. Philipson, J. J., Hillman, J. R. & Wilkins, M. B. (1973) *Planta* **11,** 87–93.
31. Rehm, M. M. & Cline, M. G. (1973) *Plant Physiol.* **51,** 93–96.
32. Berridge, M. J. & Irvine, R. F. (1989) *Nature (London)* **341,** 197–205.